

## SOME FEATURES OF THE ELECTRIC CONDUCTIVITY AND MAGNETORESISTANCE OF ANTIMONY AT LOW TEMPERATURES

Yu. A. BOGOD, B. I. VERKIN, and V. B. KRASOVITSKIĬ

Physico-technical Institute of Low Temperatures, Ukrainian Academy of Sciences

Submitted December 23, 1970

Zh. Eksp. Teor. Fiz. 61, 275-286 (July, 1971)

The previously observed singularities in the electric conductivity and magnetoresistance of antimony<sup>[7]</sup> are studied in a temperature range between 2 and 77°K for sample thicknesses between 0.5 and 4 mm. It is shown that there is a great difference between the mean free paths determined from the mobility and from the size effect (at 4 and 14°K, the difference is about one and a half orders of magnitude). It is therefore concluded that concentration gradients of macroscopic thickness develop in finite-size antimony samples located in an electric field. It is suggested that in infinite antimony samples whose purity and physical perfection are equivalent to those studied in the present work the scattering of charge carriers at 20°K is due chiefly to crystal lattice defects and to phonons.

### INTRODUCTION

AS follows from the Boltzmann kinetic equation, in the relaxation time approximation and in the absence of temperature and concentration gradients in the carrier system, the magnetoresistance effect  $\Delta R_H/R_0$  is determined by the product  $H\tau$ <sup>[1]</sup> ( $\Delta R_H/R_0 = (R_H - R_0)/R_0$ ,  $R_H$  is the electric resistance in the field  $H$ ,  $R_0$  the resistance in zero field, and  $\tau$  the relaxation time). If the relaxation time is a tensor whose principal axes coincide with the principal axes of the effective mass tensor, the indicated pair of quantities appear in all the expressions in the form of the ratio  $\tau_i/m_i$ <sup>[2]</sup> which is proportional to the mobility  $\mu_i = e\tau_i/m_i$ . Since the number of electrons in antimony is equal to the number of holes, the transverse magnetoresistance should be proportional to  $H^2$ <sup>[3]</sup>, and components of the type  $\mu_i/\mu_k H^2$  enter into the expression for  $\Delta R_H/R_0$ , while the number of components and combination of factors in the products  $\mu_i\mu_k$  will generally depend on the direction of the magnetic field.

It was discovered earlier<sup>[4,5]</sup> that in the transition from helium temperatures to hydrogen, the maximum and the minimum of the magnetoresistance effect on the angle diagrams of pure antimony single crystals in a magnetic field perpendicular to the bisector axis change places (the transverse dimensions of the samples studied amounted approximately to  $1.5 \times 1.5$  m). It is clear from what has been pointed out that, within the framework of the approximations pointed out, a similar phenomenon can be associated with the different temperature dependence both of the components of the effective mass tensor and of the relaxation time. The temperature dependence of the anisotropy of the crystal lattice can be reduced to the change in the parameters of the energy spectrum of antimony<sup>[6]</sup> and the value of the anisotropy of the relaxation time for the given parameters of the spectrum is determined by the scattering mechanism.

The decisive role of scattering mechanisms in the phenomena observed in<sup>[4,5]</sup> became clear after experiments which showed that the form of the rotation dia-

grams, which are characteristic for hydrogen temperatures, can be realized for other, different conditions and in the helium range, provided the sample thickness is sufficiently large.<sup>[7]</sup> However, the free path length of the carriers in antimony, which is obtained by the introduction of the results of studies at room temperature<sup>[8]</sup> for the conditions of the experiments in<sup>[7]</sup>, turned out to be much smaller than the sample thickness. In this connection, an assumption was made<sup>[7]</sup> concerning the diffusion origin of the size effect in antimony. Realization of a size effect of such a type indicates the presence of regions of nonequilibrium carrier distribution in the antimony samples of macroscopic thickness.<sup>[9,10]</sup>

In the present work, the previously-observed features of the electric and magnetoresistance of antimony were studied in detail in the thickness range 0.5-4 mm. This made it possible to determine the intravalley mobility qualitatively and also to estimate the diffusion path length of the carriers. Nevertheless, for unambiguous conclusions on the nature of the observed effects and for quantitative calculations, a comparison is necessary with the theories of galvanomagnetic phenomena, which are constructed with account of the appearance of transverse carrier concentration gradients in bounded semimetals placed in an electric field.

### MEASUREMENT METHOD. SAMPLES

The measurements were carried out in stationary (up to 20 kOe) and pulsed (up to 120 kOe) transverse magnetic fields. In the first case, the signal, which is proportional to the potential drop across the sample, passes through an F116/1 dc amplifier to the Y coordinate of an X-Y recorder and is registered as a function either of the current through the winding of a Kapitza electromagnet or of the direction of the transverse magnetic field. The magnet was fed from a P-62 motor-generator by means of a transistorized stabilizer, with current regulation from 0 to 100 A.<sup>[11]</sup> Automatic recording of the voltage drop across the sample

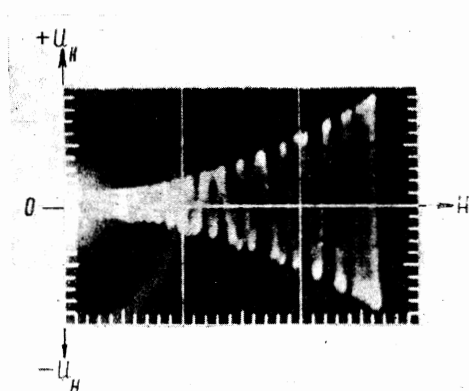


FIG. 1. Drop in potential across an antimony sample placed in a pulsed magnetic field (oscillogram).

Table I

No. of sample	Dimension, mm*	$\frac{R_0(300^\circ\text{K})}{R_0(4.2^\circ\text{K})}$
1	12 (C <sub>1</sub> ) $\times$ 1.7 (C <sub>2</sub> ) $\times$ 1.6 (C <sub>3</sub> ), h = 7	1150
4	13 (C <sub>1</sub> ) $\times$ 1.7 (C <sub>2</sub> ) $\times$ 1.8 (C <sub>3</sub> ), h = 5	1080
5	25 (C <sub>1</sub> ) $\times$ 4 (C <sub>2</sub> ) $\times$ 4 (C <sub>3</sub> ), h = 15	1650
6	21 (C <sub>1</sub> ) $\times$ 1.3 (C <sub>2</sub> ) $\times$ 1.5 (C <sub>3</sub> ), h = 15	1070
7	8.5 (C <sub>1</sub> ) $\times$ 0.5 (C <sub>2</sub> ) $\times$ 0.5 (C <sub>3</sub> ), h = 4.2	346
8	19.5 (C <sub>1</sub> ) $\times$ 2.3 (C <sub>2</sub> ) $\times$ 2.3 (C <sub>3</sub> ), h = 11	1328

\*The corresponding directions of the crystallographic axes are given in parentheses—the bisector (C<sub>1</sub>), the binary (C<sub>2</sub>) and the trigonal (C<sub>3</sub>), h is the distance between the potential contacts.

was monitored with an R-308 potentiometer with discrete application of the magnetic field and double commutation of the current and field. The current through the sample did not exceed  $5 \times 10^{-2}$  A for measurement of the electrical conductivity and  $5 \times 10^{-3}$  A for measurement of the magnetoresistance.

The pulsed magnetic field (10–120 kOe) was produced by discharging a battery of electrolytic capacitors through a small-size solenoid immersed in a cooling liquid.<sup>[12]</sup> By means of an integrating circuit inductively coupled with a coil connected in the "battery-solenoid" discharge circuit, the signal, which is proportional to the magnetic field, is plotted on the X coordinate of a double beam oscilloscope. On the Y coordinate is a signal proportional to the potential drop  $U_H$  on the sample (at a frequency of 3500 Hz). The basic criterion for the accuracy of the results of measurement in pulsed fields was a comparison of the results with the data obtained in a constant field. A typical oscillogram of  $U_H = f(H)$  is shown in Fig. 1.

The temperature regulation was achieved by pumping off liquid helium and hydrogen, and also with the aid of a heater, mounted with the sample and the temperature pickup in an ampoule filled with gaseous helium. When using the heater, the temperature was stabilized by an electronic stabilizer, which guaranteed its constancy with an accuracy to within  $0.001^\circ$  in the helium region, and  $0.1^\circ$  in the hydrogen region. As a pickup for the stabilization and for the temperature measurement, we used a carbon resistor of the Allen Bradley type with a sensitivity of  $R^{-1}DR/dT = 0.5 \text{ deg}^{-1}$  at  $4.2^\circ\text{K}$ .

The antimony samples were cut with an electric-

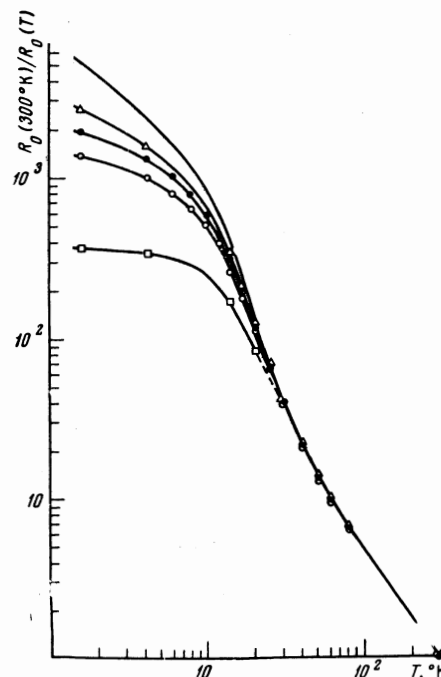


FIG. 2. Temperature dependence of the electric conductivity of antimony single crystals. The symbols  $\Delta$ ,  $\bullet$ ,  $\circ$ ,  $\square$  corresponds to samples 5, 6, 7, 8. The upper curve (without the circles) was constructed for a sample of infinite thickness.

spark cutter from two monocrystalline ingots of different batches; samples 1 and 4 were from one ingot and samples 5–8 from the other, and had the shape of bars with square or almost square transverse cross section. The longitudinal axis of the bars was parallel to C<sub>1</sub>, the current and potential contacts were supplied by copper conductors and attached by lead-tin solder.

The characteristics of the investigated crystals are given in Table I.

## EXPERIMENTAL RESULTS

### 1. Electrical Conductivity

Figure 2 shows the temperature dependence of the ratio  $R_0(300^\circ\text{K})/R_0(T) \sim \sigma_0(T)$  for samples 5–8. It is seen that, in the range 1.6– $30^\circ\text{K}$ , upon decrease in the sample thickness, the value of the conductivity  $\sigma_0(T)$  also decreases, and the decrease increases with decreasing temperature. Graphical extrapolation into the region of infinite thickness ( $d \rightarrow \infty$ ) expressed in the coordinates  $R_0(T)/R_0(300^\circ\text{K}) - 1/d$ , makes it possible to obtain the temperature dependence of the conductivity without account of the boundary effects (see the upper curve in Fig. 2). As  $d \rightarrow \infty$  below  $10^\circ\text{K}$ , there is region of residual conductivity and in the region 10– $30^\circ\text{K}$ ,  $\gamma_0(T) \sim T^{-3 \pm 0.2}$ . For the range 77– $300^\circ\text{K}$ , the electrical conductivity falls off according to the law  $\sigma_0(T) \sim T^{-1/4}$ .

### 2. Magnetoresistance

Figure 3 shows a copy of the recording of the angular diagram of antimony crystals in a magnetic field, taken for the temperature 1.6 and  $20^\circ\text{K}$ . It is seen that both increase in temperature and increase in the transverse dimensions of the sample lead to rotation dia-

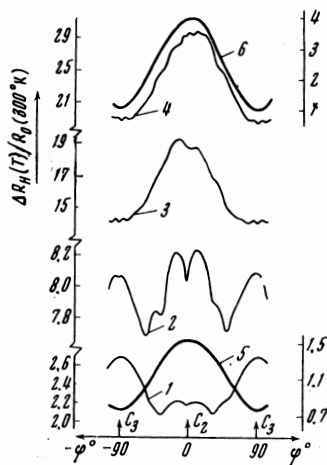


FIG. 3. Rotation diagrams of antimony single crystals in a magnetic field  $H = 15$  kOe. Curves 1, 2, 3, 4 refer to the samples 7, 6, 8, 5;  $T = 1.6^\circ\text{K}$ . Curves 5 and 6—samples 7 and 5,  $T = 20.4^\circ\text{K}$  (scale at the right).

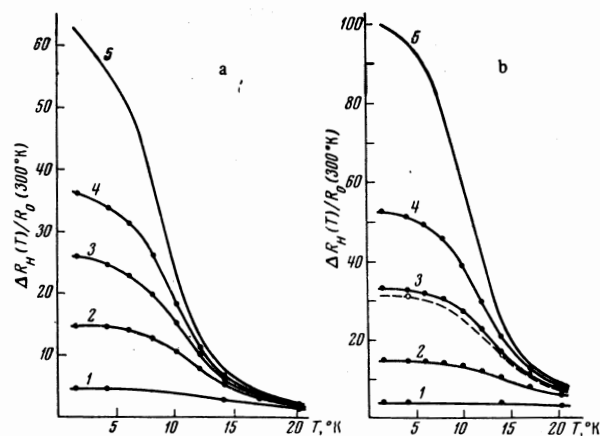


FIG. 4. Temperature dependence of the magnetoresistance of antimony for crystals with thickness: 1—0.5 mm, 2—1.3 mm, 3—2.3 mm, 4—4 mm. Curve 5 (without the circles) gives the extrapolation to  $d \rightarrow \infty$  for  $H = 20$  kOe. a— $H \parallel C_3$ ; b— $H \parallel C_2$ ; the dashed curve shows the curve for sample 9 (see Table III).

grams of the same type with a maximum for  $H \parallel C_2$  and minimum for  $H \parallel C_3$ ; the effect of the thickness on the value of the magnetoresistive effect is greater than in the case  $H \parallel C_3$ . The same also follows from the curves of the temperature dependence of the magnetoresistance (Fig. 4,  $\Delta R_H(T) = R_H(T) - R_0(T) \approx R_H(T)$ ). Here the function  $\Delta R_H(T)/R_0(300^\circ\text{K})$  falls off more slowly the thinner the sample, which is especially significant for  $H \parallel C_2$ . The temperature dependence of the magnetoresistance as  $d \rightarrow \infty$  (Fig. 4) was determined by extrapolation, as in the case of the conductivity (Fig. 5).

In the study of the dependence of the resistance on the magnetic field, that temperature region was first found in which the resistance for the given values of  $H$  (5–20 kOe) is described by a single power dependence of the form

$$\Delta R_H(T) / R_0(T) = \beta(T) H^{n(T)}. \quad (1)$$

For this purpose the function

$$f = \lg \frac{\Delta R_{H_i}(T)}{\Delta R_{H_k}(T)} / \lg \frac{\Delta R_{H_i}(T)}{\Delta R_{H_l}(T)}, \quad (2)$$

was chosen. This function is a straight line parallel

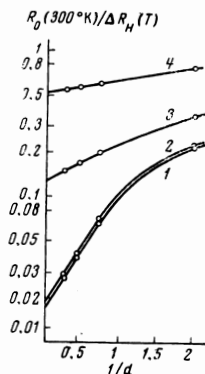


FIG. 5

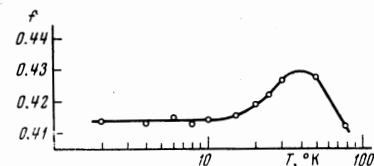


FIG. 6

FIG. 5. Determination of the magnetoresistance of a sample of infinite thickness for  $H \parallel C_3$  and temperature: 1—1.6, 2—4.2, 3—14, 4—20.4°K in a magnetic field  $H = 20$  kOe.

FIG. 6. Dependence of the function  $f$  on the temperature: indices  $i$ ,  $k$  and  $l$  in Eq. (2) correspond to the values of  $H$  equal to 20, 15 and 10 kOe.

Table II

d, mm	$T = 4.2^\circ\text{K}$		$T = 14^\circ\text{K}$	
	$H \parallel C_2$	$H \parallel C_3$	$H \parallel C_2$	$H \parallel C_3$
4	1.82	1.95	1.94	2.0
2.3	1.78	1.93	1.91	1.98
1.3	1.77	1.86	1.83	1.92
0.5	1.67	1.72	1.67	1.8

to the  $T$  axis when (1) is plotted in the coordinates  $f$  and  $T$  (the indices  $i$ ,  $k$ , and  $l$  correspond to the different values of the field). As measurements have shown, the variation in the magnetoresistance in the range 5–20 kOe is well described by the formula (1) only when  $T < 15^\circ\text{K}$  (Fig. 6). We have assumed that the deviations from the law (1) for  $T > 15^\circ\text{K}$  are due to the too small values of  $H$ . Actually, from experiments carried out with pulsed fields, it follows that in the range 20–120 kOe, for  $T = 20.4^\circ\text{K}$ , the magnetoresistance is well described by the function (1) with the exponent  $n = 2$ .

At helium temperatures and for samples 1 and 4, the exponent is equal, correspondingly, to

$$n = \begin{cases} 1.78; 1.8 & \text{for } H \parallel C_2, \\ 1.85; 1.86 & \text{for } H \parallel C_3. \end{cases}$$

(with accuracy to within  $\pm 0.02$ ; in pulsed magnetic fields, for crystal 4, we obtained  $n = 1.78$  for  $H \parallel C_2$  and  $n = 1.83$  for  $H \parallel C_3$ ). These results are in satisfactory agreement with the values of  $n$  of antimony samples of corresponding thicknesses from the other batch (see Table II, in which the values of  $n$  are given for  $T = 4.2^\circ\text{K}$  and  $14^\circ\text{K}$ . These correspond to different thicknesses and directions  $H \parallel C_2$  and  $H \parallel C_3$ ). As is seen from the table, the exponent depends on the orientation of  $H$  relative to the axes of the crystal and for a given thickness, its value for the case  $H \parallel C_3$  is greater than for the case  $H \parallel C_2$ . Besides, the value of  $n$  increase with increase in the transverse dimen-

sions of the sample and approaches 2 on going from low to high temperatures.<sup>1)</sup>

## DISCUSSION OF RESULTS

### 1. Free Path Length of Carriers in Antimony

As shown in<sup>[9,10]</sup>, the electrons in semiconductors and semimetals with multivalley structure of the energy spectrum undergo two forms of collisions, which characterize the change in the momentum—intravalley (with relaxation time  $\tau$ ) and intervalley (with relaxation time  $\tau$ ). The probability of collisions leading to intervalley transitions falls off exponentially upon decrease in temperature, with an activation energy of the order of the Debye energy  $k\Theta_D$ , so that,  $\tau \ll \tau_M$  for  $T \ll \Theta_D$ . Therefore, for low temperatures in an unbounded semimetal, the effect of intervalley transitions on the kinetic coefficients is negligibly small. However, when the electric current flows through a bounded plate of a multivalley semimetal, the equilibrium distribution of the electrons in the layer near the surface is disturbed, owing to the different inclinations of the equal-energy quasiellipsoids of the various valleys to the boundary surface. For large values of  $\tau_M$  the concentration gradients that are formed spread out weakly and can have macroscopic thickness. Such a system (for not too large intervalley scattering by the surface), according to<sup>[9,10]</sup>, should lead to size effects of a new type, generated by a diffusion path length  $L \approx v_F \sqrt{\tau \tau_M}$  which, at  $T \ll \Theta_D$ , appreciably exceeds the ordinary (intravalley) path length  $l \approx v_F \tau$ .

The value of  $l$  can be determined from measurements of the mobility. The discrepancy between the path length determined in this manner and the path length obtained from data on the size effect would appear to confirm that the phenomena predicted in<sup>[9,10]</sup> are realized in semimetals.

An interpretation of the experimental results in the present work was also carried out within the framework of such a scheme. Here we used a two-band model of the energy spectrum with a quadratic and isotropic dispersion law for each band. The model described above is far from the real energy spectrum of antimony,<sup>[13]</sup> therefore the corresponding calculations are naturally not a quantitative analysis and have the character of qualitative estimates.

The initial data for the calculation was obtained by graphical extrapolation of the magnetoresistance (for  $H \parallel C_3$ ,  $H = 20$  kOe) and the conductivity in the range of infinite thicknesses, which allowed us to eliminate the effect of the boundary. The intravalley mobilities of the carriers ( $\mu_1$  and  $\mu_2$ ) were obtained from the equations

$$\Delta \rho_H(T) / \rho_0(T) = \mu_1 \mu_2 H^2, \quad 1 / \rho_0(T) = Ne(\mu_1 + \mu_2), \quad (3)$$

where  $N = 5.36 \times 10^{19} \text{ cm}^{-3}$ <sup>[14]</sup> is the concentration of

<sup>1)</sup>By obtaining graphically the magnetoresistance of a sample of infinite thickness (see Fig. 5) for various values of  $H$ , we have established the fact that, in the temperature range 1.6–14°K and  $d \rightarrow \infty$ , the resistance increases quadratically in the magnetic field, i.e.,  $n = 2$ . (The error in such a procedure of determining the exponent is connected with the errors of extrapolation and is not less than 20%.)

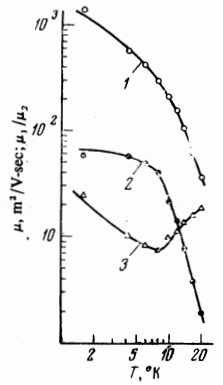


FIG. 7. Temperature dependence of the mobilities  $\mu_1$  and  $\mu_2$  (curve 1 and 2) and their ratio (curve 3).

electrons in Sb (equal to the concentration of holes  $P$ ),

$$\frac{\Delta \rho_H(T)}{\rho_0(T)} = \frac{R_0(300^\circ\text{K})}{R_0(T)} \frac{R_0(300^\circ\text{K})}{\Delta R_H(T)}$$

$$\rho_0(300^\circ\text{K}) = 42.6 \cdot 10^{-6} \text{ ohm-cm,}$$

Figure 7 shows the temperature dependence of the mobilities in the interval 1.6–20.4°K. If the effective mass of the carriers remains constant upon variation of  $T$ , the temperature dependence of the relaxation times  $\tau_1$  and  $\tau_2$ , which characterize the change in momentum, will have the same shape.

For an estimate of the path length  $l$  associated with intervalley collisions, we used the values of the mobility  $\mu_2$ , setting the corresponding effective mass equal to the mass of the free electrons, and assuming a Fermi velocity  $v_F \approx 2 \times 10^7$  cm/sec.<sup>[15,16]</sup>

The characteristic path length that gives rise to the size effects ( $L$ ) was determined from the curve of the temperature dependence of the magnetoresistance. It was assumed here that  $\Delta R_H(T) = \text{const}$  when  $L \geq d$ . The curves obtained for  $H \parallel C_2$  and equal to 0.5 and 1.3 mm turned out to be most suitable for such a procedure (see Fig. 4b). As a result, we obtained

$$T = 4^\circ\text{K}: l \approx 7 \cdot 10^{-3} \text{ cm}, L \approx 1.3 \cdot 10^{-1} \text{ cm};$$

$$T = 14^\circ\text{K}: l \approx 1 \cdot 10^{-3} \text{ cm}, L \approx 0.5 \cdot 10^{-1} \text{ cm.}$$

It must be taken into account that the values of  $l$  are apparently too high by several times because of the value attributed to the effective mass of the carriers with mobility  $\mu_2$ . Thus the path lengths in antimony determined from the mobility and from the size effect differ by about one and one half orders of magnitude, which can be connected with the presence in the antimony samples of regions, of macroscopic thickness, of nonequilibrium distribution of the carriers.<sup>2)</sup>

The problem of the nonequilibrium charge distribution in the near-surface layer of compensated semimetals was considered in the works of Japanese authors,<sup>[18-20]</sup> who studied the kinetic properties of bismuth. The reason for the appearance of the concentration gradients in the above-mentioned works is the

<sup>2)</sup>The lack of agreement of the path lengths determined from the mobility and from the size effect was noted by Freedman in a study<sup>[17]</sup> of the electric conductivity of bismuth. The size effects led to values of the path lengths that were several times greater. Gorkun and Rashba pointed out a possible connection between the phenomenon noted in<sup>[17]</sup> and the generation of carrier concentration gradients in the Bi.<sup>[19]</sup>

Table III

No. of sample	Cross section, mm <sup>2</sup>	$\frac{R_0(300^\circ\text{K})}{R_0(4.2^\circ\text{K})}$	$\frac{\Delta H \cdot C_s}{H \parallel C_s}$ H = 20 kOe	n	
				H $\parallel$ C <sub>s</sub>	H $\perp$ C <sub>s</sub>
5	4×4	1650	1.5	1.82	1.95
6	1.3×1.3	1070	0.97	1.77	1.86
9	0.9×1.1	1220	1.1	1.87	2.0

bipolar drift of the carriers which arises under the action of the external magnetic field or the magnetic field of the current. The linear volt-ampere characteristics, measured in the present work in the range  $10^{-2} - 3 \times 10^{-1}$  A at helium temperatures put such viewpoint under some doubt in any case as applied to antimony.<sup>3)</sup>

Amplification processes can exert an influence on the size effect in semimetals:<sup>[22]</sup> as soon as the thickness of the sample becomes comparable with the path length  $l_{ph}$  of the nonequilibrium phonons carried along by the electrons, the distribution function of the phonons relaxes rapidly, which leads to the liquidation of the amplification processes, and, consequently, to a change in the conductivity. In such a system, at least in the region of the size effect ( $l_{ph} \leq d$ ), when the system of phonons is in equilibrium, the resistance of the compensated semimetal should grow in proportion with the square of the field, which is entirely counter to the results of the present research. Therefore, the influence of the amplification processes on the size effect in antimony is hardly significant.

## 2. Effect of the method of sample preparation on the kinetic properties of antimony.

In the concluding phase of the present work, a check was made on the effect on the results of the experiments of the method of sample preparation. Bars were cut from the same ingot as samples 5–8. These bars had a cross section of  $3 \times 3$  mm. By etching techniques, the cross section was reduced to  $0.9 \times 1.1$  mm. It is seen (see Fig. 4b and Table III) that the effect of the dimensions on the kinetic properties of sample 9 obtained in this way was less than in the case of sample 6.

Let us consider the structure features of antimony samples produced by an electric spark cutter and discuss their effect on the electrical conductivity. The electric spark cutting of the antimony produced, in addition to defects in the surface layer, also twins (with twinning planes of the type  $\{101\}$ ) that penetrated to a depth of several mm. The widths of the twin regions usually amounted to  $\sim 10^{-3}$  cm, and the distance between them varied in the range  $5 \times 10^{-1} - 5 \times 10^{-2}$  cm. Therefore, the change in the electrical and magnetoresistance brought about by the disorientation of the twin regions relative to the parent part of the crystal cannot amount to more than several per cent.

When account is taken of the influence of faulty electric spark cutting of the surface layer on the kinetic properties of antimony, serious difficulties develop because of the absence of data on its depth and struc-

ture. If we assume a layer thickness  $\sim 10^{-3}$  cm<sup>4)</sup> and that the specific values of the electric and magnetoresistance are of the same order as in the core of the sample, then the removal of a layer can lead to an increase in the ratio  $R_H(4.2^\circ\text{K})/R_0(300^\circ\text{K})$  of sample 6 by 1–10% (this follows from where the core and surface layer are regarded as two conductors connected in parallel). However, the difference in the quantities  $R_H(4.2^\circ\text{K})/R_0(300^\circ\text{K})$  for samples 6 and 9 is much greater—from 70 to 100% for different directions of the magnetic field. Nevertheless, the degree of influence of the damaged layer is not finally clear. In this connection, it may be suggested that the observed size effects may be a consequence of the dissimilar state of the crystal lattice in samples of different thickness prepared by the electric spark cutter. Comparison of the results obtained with samples 5 and 9 (see Fig. 4b and Table III) shows that the ratio  $R_0(300^\circ\text{K})/R_0(4.2^\circ\text{K})$ , and also the quantity  $R_H(4.2^\circ\text{K})/R_0(300^\circ\text{K})$  of sample 6, exceed the values of the corresponding quantities measured on sample 9, which was obtained by etching to a depth of  $\sim 1$  mm and known beforehand not to have defects in the surface layer, even if it is assumed that in electric spark treatment the defects penetrate to a depth of  $\sim 0.1$  mm<sup>5)</sup>. On the other hand, it is clear that the presence in sample 5 of a defective surface layer can only decrease the quantities indicated above. Thus the influence of the size effect on the kinetic properties is subject to no doubt. This is also confirmed by measurements of the electric conductivity and magnetoresistance of samples whose thickness was varied by chemical etching.

The essential difference in the kinetic properties of the antimony samples which have close geometric dimensions but are prepared by different methods (electric spark cutting and chemical etching), observed in the present research, can be accounted for, in the opinion of the authors, in addition to the unaccounted for effect of the surface layer, by two not mutually exclusive reasons—scattering by boundary twins and the different states of the surface. These questions are being investigated at the present time.

## 3. Mechanisms of Scattering in Infinitely Thick Antimony Samples

As was pointed out above, in an unbounded semimetal the effect of the intervalley transitions on the kinetic coefficients at low temperatures is negligibly small, so that the relaxation of the distribution function of the electrons is realized fundamentally through intravalley collisions.

Let us consider what are the possible temperature dependences of the intravalley relaxation times of two groups of carriers in antimony if the effective masses of the carriers of the different types are essentially different. For sufficiently low temperatures, the scattering is basically due to static defects, and in the simplest case of an elastic and isotropic scattering the relaxation times are constant and the free path

<sup>3)</sup>The linearity of the volt-ampere characteristics of antimony samples of cross section  $1.5 \times 1.5$  mm, up to values of  $J = 7$  A, follows from [21].

<sup>4)</sup>According to the data obtained on molybdenum and tungsten. [23]

<sup>5)</sup>Such is the depth of the plastically deformed layer in electric spark treatment of copper. [24]

lengths are equal to one another. As the temperature increases, in the transition to scattering from phonons, the relaxation times characterizing the change in the momentum begin to decrease; this is the more intense for groups for which there is a probability of scattering at large angles. Then, if the momentum of the carriers of the small group is such that each scattering act becomes "effective," i.e., the scattering angle is  $\geq \pi/2$  (in antimony for minimum Fermi momentum  $p_F$  this can occur at a temperature  $\sim 2p_F s/k \approx 5^\circ\text{K}$ , where  $s$  is the sound velocity), the corresponding relaxation time  $\tau$ , falls off in inverse proportion to the number of phonons. For  $T \ll \Theta_D$ , we have  $\tau_1 \sim 1/T^3$ . For heavy carriers under these same conditions, the scattering angle is  $< \pi/2$  and, consequently,  $\tau_2 \sim 1/T^5$ . In antimony, the maximum effective Debye temperature for the electron-phonon (intravalley) interaction  $\Theta_D^*$  is also not large, only  $25^\circ\text{K}$ ,<sup>[25]</sup> so that  $\tau_2 \sim 1/T^5$  within the framework of the assumptions made, when  $T \ll 25^\circ\text{K}$ .

The model considered describes the experimental results qualitatively. Actually, when  $1.6 < T < 10^\circ\text{K}$ , the intravalley mobilities depend weakly on the temperature, and the rate of change of  $\mu_2$  ( $\mu_2 \ll \mu_1$ , see Fig. 7) is much less than that of  $\mu_1$ . In the range  $10-20^\circ\text{K}$ ,  $\mu_1 \sim 1/T^{2.8}$ , so that the temperature dependence of  $\tau_1$  is close to inverse cubic. For the second group of carriers in the range  $10-20^\circ\text{K}$ ,  $\tau_1 \sim 1/T^4$  (Fig. 7). Here the deviation from the law  $1/T^5$  is most probably associated with the loose satisfaction of the condition  $T \ll \Theta_D$  in the indicated temperature region, which can be extended in the direction of lower temperatures only by using more perfect specimens. Thus, we are inclined to assume that in infinite antimony samples whose purity and physical perfection are equivalent to those studied in the present research, in the temperature range  $1.6-20^\circ\text{K}$ , the relaxation of the distribution function of the carriers is due mainly to lattice defects and to phonons. We also note that the unequal temperature dependences of the mobilities  $\mu_1$  and  $\mu_2$  indicates the non-fulfillment of Kohler's rule in antimony, at least in the temperature region studied.

We now compare our results with the data of Red'ko, Bresler, and Shalyt,<sup>[26]</sup> who studied the law of Wiedemann and Franz for an antimony single crystal with longitudinal axis parallel to  $C_3$ , the ratio  $R_0(300^\circ\text{K})/R_0(4.2^\circ\text{K}) = 2500$  and the area of the transverse cross section  $2 \times 2.5$  mm. In particular, it has been shown by the authors<sup>[26]</sup> that, in the interval  $2-10^\circ\text{K}$ , the Wiedemann-Franz law is not satisfied, and in the vicinity of  $4^\circ\text{K}$  the curve  $\mathcal{L}(T) = \kappa/\sigma T$  has a minimum.

In the model assumed in the present work,  $\kappa \sim (\tau' + \tau'')/T$ , where  $\tau'$  and  $\tau''$  are the relaxation times of two groups of the carriers; they characterize the change in the energy and are proportional to  $1/T^3$  for  $T \ll \Theta_D$ . In correspondence with what was said above, in the scattering by static defects and phonons, the relaxation times characterizing the processes of thermal conductivity and electric conductivity of the small group of carriers coincide and

$$\mathcal{L}(T) \sim [1 + \mu_2(T)/\mu_1(T)]^{-1}. \quad (4)$$

Thus the shape of the function  $\mathcal{L}(T)$  is determined by

the ratio of the mobilities of the large and small group.

As is seen from Fig. 7, the ratio  $\mu_1/\mu_2$  in the vicinity of  $8^\circ\text{K}$  and consequently the dependence  $\mathcal{L}(T)$ , have a minimum. This agrees qualitatively with the results of<sup>[26]</sup> which indicates the presence in the antimony of an inelastic scattering mechanism for  $T < \Theta_D^* = 25^\circ\text{K}$ .

Up to the present time, the classical galvanometric effects in antimony have as a rule been studied in the range of temperatures  $77-300^\circ\text{K}$ .<sup>[8,27-29]</sup> so far as the region of much lower temperatures is concerned, only one research of this type is known to us, carried out at helium temperatures on sufficiently pure single crystalline samples.<sup>[30]</sup> The interpretation of the results of<sup>[30]</sup> was carried out within the framework of the two-band model. The electric field applied to the sample was parallel to the  $C_2$  axis. Numerical values of the mobilities, obtained for  $T = 4.2^\circ\text{K}$  in<sup>[30]</sup> and in the present research are respectively equal to

$$\mu_1 = 1 \cdot 10^2 \text{ m}^2/\text{V-sec} \quad [30], \quad 5.6 \cdot 10^2 \text{ m}^2/\text{V-sec} \text{ present work}$$

$$\mu_2 = 0.2 \cdot 10^2 \text{ m}^2/\text{V-sec} \quad [30], \quad 0.56 \cdot 10^2 \text{ m}^2/\text{V-sec} \text{ present work}$$

For  $T = 20.4^\circ\text{K}$ , according to our data,  $\mu_1 = 36 \text{ m}^2/\text{V-sec}$ , and  $\mu_2 = 1.9 \text{ m}^2/\text{V-sec}$ . This agrees with the values  $H_0^{(1)} \approx 280$  Oe and  $H_0^{(2)} \approx 5000$  Oe. (When  $H = H_0^{(1)}$ , the radius of the orbit of carriers of type i is equal to the free path length  $l$ .)

Thus, the condition  $H \gg H_0$  for heavy carriers in antimony is satisfied for hydrogen temperatures only in fields of several dozen kOe. It is evident that this is the reason for the deviation of the magnetoresistance at  $T > 15^\circ\text{K}$  and  $5 \text{ kOe} < H < 20 \text{ kOe}$  (Fig. 6) from the single power-law dependence, that is usually observed in strong ( $H \gg H_0$ ) magnetic fields.

<sup>1</sup>J. Ziman, *Electrons and Phonons*, (Oxford, 1961).

<sup>2</sup>C. Herring and E. Vogt, *Phys. Rev.* 101, 944 (1956).

<sup>3</sup>I. M. Lifshitz, M. Ya. Azbel' and M. I. Kaganov, *Zh. Eksp. Teor. Fiz.* 31, 63 (1956) [*Sov. Phys.-JETP* 4, 41 (1957)].

<sup>4</sup>Yu. A. Bogod and V. V. Eremenko, *Zh. Eksp. Teor. Fiz.* 53, 473 (1967) [*Soviet Phys.-JETP* 26, 311 (1968)].

<sup>5</sup>Yu. A. Bogod and V. B. Krasovitskiĭ, *Phys. Stat. Solidi* 40, K55 (1970).

<sup>6</sup>G. V. Bunton and S. Weintraub, *J. Phys. (Proc. Phys. Soc.)* C2, 116 (1969).

<sup>7</sup>Yu. A. Bogod, B. I. Verkin, and V. B. Krasovitskiĭ, Preprint, Physico-technical Institute of Low Temperatures, Academy of Sciences, Ukrainian SSR, 1970; Yu. A. Bogod, B. I. Verkin and B. V. Krasovitskiĭ, *ZhETF Pis. Red.* 12, 224 (1970) [*JETP Lett.* 12, 155 (1970)].

<sup>8</sup>Ö. Öktü and G. A. Saunders, *Proc. Roy. Soc. (London)* 91, 156 (1967).

<sup>9</sup>E. I. Rashba, *Zh. Eksp. Teor. Fiz.* 48, 1427 (1965) [*Soviet Phys.-JETP* 21, 954 (1965)].

<sup>10</sup>Yu. I. Gorkun and É. I. Rashba, *Fiz. Tverd. Tela* 10, 3053 (1968) [*Soviet Phys.-Solid State* 10, 2406 (1969)].

<sup>11</sup>V. M. Naumenko and B. G. Rudenko, *PTÉ* No. 2, 150 (1968).

<sup>12</sup>Yu. A. Bogod, Candidate's Dissertation, Physico-technical Institute of Low Temperatures, Academy of Sciences, Ukrainian SSR, 1968).

- <sup>13</sup>L. M. Falicov and P. J. Lin, Phys. Rev. 141, 562 (1966).
- <sup>14</sup>L. R. Windmiller and M. G. Priestley, Solid State Comm. 3, 199 (1965).
- <sup>15</sup>Y. E. Eckstein, Phys. Lett. 20, 142 (1966).
- <sup>16</sup>A. P. Korolyuk and L. Ya. Matsakov, ZhETF Pis. Red. 3, 291 (1966) [JETP Lett. 3, 188 (1966)].
- <sup>17</sup>A. N. Freedman, Phys. Rev. 159, 158 (1967).
- <sup>18</sup>S. Tanuma and Y. Ichizava, X Intern. Conf. on Low Temperature Physics, Moscow, 1967.
- <sup>19</sup>R. N. Zitter, Phys. Rev. Lett. 14, 14 (1965).
- <sup>20</sup>T. Hattori, J. Phys. Soc. Jap. 23, 19 (1967).
- <sup>21</sup>Yu. A. Bogod, and V. B. Krasovitskiĭ, ZhETF Pis. Red. 7, 301 (1968) [JETP Lett. 7, 235 (1968)].
- <sup>22</sup>J. E. Aubrey and C. J. Greasy, J. Phys. C (Solid State Phys.) 2, 824 (1969).
- <sup>23</sup>P. Beardmore and D. Hull, J. Inst. Metals 94, 14 (1966).
- <sup>24</sup>W. T. Brydges, J. Inst. Metals 95, 223 (1967).
- <sup>25</sup>R. S. Blewer, N. H. Zebouni, and C. G. Grenier, Phys. Rev. 174, 700 (1968).
- <sup>26</sup>N. A. Red'ko, M. S. Bresler and S. S. Shalyt, Fiz. Tverd. Tela 11, 3005 (1969) [Sov. Phys.-Solid State 11, 2435 (1970)].
- <sup>27</sup>S. J. Freedman and H. J. Juretschke, Phys. Rev. 124, 1379 (1961).
- <sup>28</sup>S. Epstein and H. J. Juretschke, Phys. Rev. 129, 1148 (1963).
- <sup>29</sup>V. V. Kechin, A. I. Likhter, and Yu. A. Pospelov, Zh. Eksp. Teor. Fiz. 49, 36 (1965) [Sov. Phys.-JETP 22, 26 (1966)].
- <sup>30</sup>G. N. Rao, N. H. Zebouni, C. G. Grenier, and J. M. Reynolds, Phys. Rev. 133, A141 (1964).

Translated by R. T. Beyer

28